

## Thermal and electrical properties of manganese (II) oxalate dihydrate and cadmium (II) oxalate monohydrate

A.K. Nikumbh\*, A.E. Athare, S.K. Pardeshi

*Department of Chemistry, University of Pune, Ganeshkhind, Pune 411007, India*

Received 4 May 1998; received in revised form 14 September 1998; accepted 22 October 1998

### Abstract

The thermal decomposition of  $\text{MnC}_2\text{O}_4 \cdot 2\text{H}_2\text{O}$  and  $\text{CdC}_2\text{O}_4 \cdot \text{H}_2\text{O}$  have been studied by two probe direct current electrical conductivity measurements under the atmospheres of static air, dynamic dry nitrogen and dynamic air. The products at each decomposition stage have been characterized by infrared spectroscopy and X-ray powder diffraction. The electrical conductivity measurements were found to give additional information on the solid-state reaction as compared to that obtained from conventional thermal analytical techniques (such as TG and DTA). © 1999 Elsevier Science B.V. All rights reserved.

*Keywords:* Electrical conductivity; Electrochemical analysis; Thermal decomposition; Oxalates; Solid-state reaction

### 1. Introduction

The thermal decomposition of metal oxalate complexes have been studied by numerous workers. The decomposition of oxalate complexes is usually complicated and occurs in a series of steps. The most obvious change is caused by the environment when the actual product is different due to the influence of the surrounding as atmosphere. The different oxide products were obtained in case of manganese (II) oxalate dihydrate ( $\text{MnC}_2\text{O}_4 \cdot 2\text{H}_2\text{O}$ ); the exact nature of the product depending on experimental conditions is an example that may be cited in literature [1–7]. The decomposition of cadmium (II) oxalate ( $\text{CdC}_2\text{O}_4 \cdot \text{H}_2\text{O}$ ) in air or an inert atmosphere leads to the formation of CdO has also been reported in literature [7,8]. However, the thermal decomposition of  $\text{MnC}_2\text{O}_4 \cdot 2\text{H}_2\text{O}$

and  $\text{CdC}_2\text{O}_4 \cdot \text{H}_2\text{O}$  by using direct current electrical conductivity measurement has not been investigated yet. This paper deals with a systematic change of electrical properties as well as that of ambient atmospheres on thermal decomposition of the  $\text{MnC}_2\text{O}_4 \cdot 2\text{H}_2\text{O}$  and  $\text{CdC}_2\text{O}_4 \cdot \text{H}_2\text{O}$ . This study has been supplemented with X-ray powder diffraction and infrared spectroscopy.

### 2. Experimental

$\text{MnC}_2\text{O}_4 \cdot 2\text{H}_2\text{O}$  and  $\text{CdC}_2\text{O}_4 \cdot \text{H}_2\text{O}$  were prepared using the methods described in literature [9,10]. Elemental and the thermal analyses confirms the presence of water of hydration; and the polymeric octahedral structure have been assigned by infrared spectra [11] for these compounds.

The procedure used for measurements of direct current electrical conductivity, infrared spectroscopy

\*Corresponding author. Tel.: +91-1457719; fax: +91-0212-353899; e-mail: aknik@unipune.in

and X-ray powder diffraction were similar to those reported earlier [12,13].

### 3. Results and discussion

#### 3.1. Static air atmosphere

##### 3.1.1. $MnC_2O_4 \cdot 2H_2O$

The temperature variation of the electrical conductivity,  $\sigma$ , (Fig. 1(a)) did not show initial decrease in conductivity (Region B') up to 95°C. Then there was a constant conductivity between 95° and 226°C (Region B). The  $\sigma$  value started to increase from 226° to 312°C (Region C), followed by a decrease and then sharp increase in  $\sigma$  up to 350°C (Region D). Later,  $\sigma$  remained almost constant in the temperature range 350–400°C (Region E).

A comparison of thermal analysis (TG and DTA) [6–8] with conductivity analysis in static air of  $MnC_2O_4 \cdot 2H_2O$  shows that the conductivity analysis gives a much more detailed view of the decomposition process. TG shows a continuous mass loss around 100–150°C with a plateau up to 220°C [6–8]. DTA

gives an endothermic peak at 130°C corresponding to dehydration of  $MnC_2O_4 \cdot 2H_2O$ ; a broad exothermic peak at 270°C corresponding to the oxidative decomposition of  $MnC_2O_4$ . The TG curve showed a continuous weight loss from 230°C until final recrystallization to  $Mn_3O_4$ . Due to the broadness of the exothermic peak in the DTA curve and to the continuous weight loss in the TG curve, the various meta-stable intermediates formed during this oxidative decomposition step could not be determined in detail. However, the direct current electrical conductivity, represented in Fig. 1(a), gave complete information on the intermediates by showing different region of conductivity.

At B' in Fig. 1(a) there was no observable change in X-ray diffraction pattern and infrared spectrum. This indicates the desorption of physically adsorbed water molecules on the upper surface of the particles. In the temperature range corresponding to Region B, the infrared spectrum revealed no  $H_2O$  peak, while the X-ray powder diffraction pattern generally showed polycrystallinity with a decrease in inter-planar spacings [14]. The elemental analysis agreed with the formula  $MnC_2O_4$ .

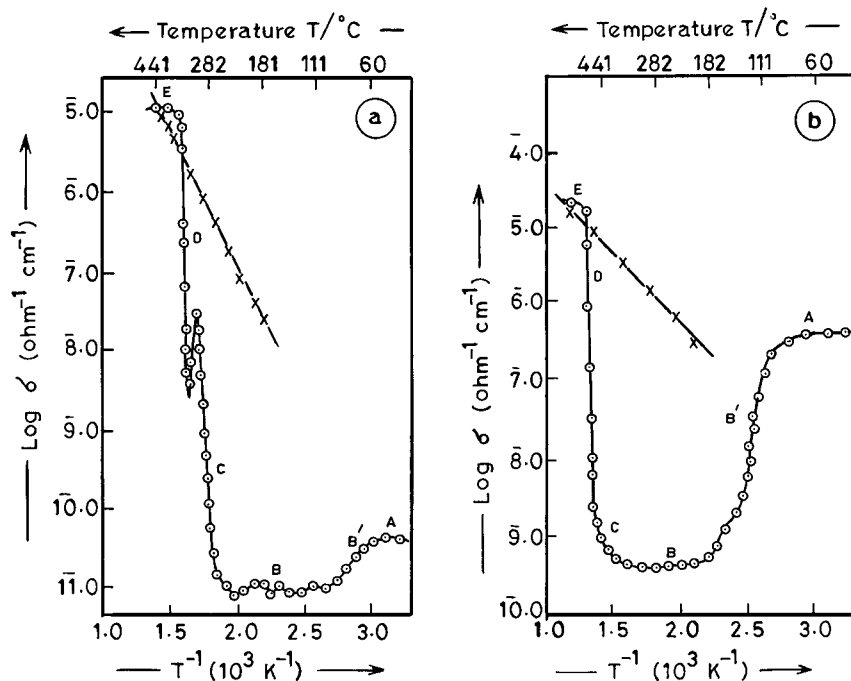


Fig. 1. Plot of  $\log \sigma$  vs.  $T^{-1}$  for (a)  $MnC_2O_4 \cdot 2H_2O$  and (b)  $CdC_2O_4 \cdot H_2O$ .  $\odot$ , during decomposition;  $\times$ , cooling cycle.

In the temperature range corresponding to Region C in Fig. 1(a), the infrared spectra showed wide changes. When  $\text{MnC}_2\text{O}_4 \cdot 2\text{H}_2\text{O}$  was heated isothermally at  $290^\circ\text{C}$ , the infrared spectrum showed a decrease in the intensities of the coordinated oxalate bands, and bands occurred at  $604\text{ cm}^{-1}$  (m) and  $475\text{ cm}^{-1}$  (m) for the M–O stretching frequencies due to the presence of the manganese oxide formed [15]. The X-ray diffraction pattern indicate that this sample was polycrystallite in nature; peaks corresponding to both MnO and  $\text{MnC}_2\text{O}_4$  were observed. Although a tendency for a sharp increase in  $\sigma$  was observed at  $331^\circ\text{C}$  (Region D), the characteristic high  $\sigma$  value of  $\text{Mn}_3\text{O}_4$  ( $\sim 10^{-5}\ \Omega^{-1}\text{ cm}^{-1}$ ) could not be obtained under dynamic conditions. However, the X-ray diffraction studies confirmed mainly to  $\text{Mn}_3\text{O}_4$  and traces of MnO were formed at this temperature. The infrared spectrum of the parent sample heated at  $340^\circ\text{C}$  showed no bands due to coordinated carboxylate, but strong bands of Mn–O stretching frequencies were observed. A sample in Region E in Fig. 1(a) was predominantly  $\text{Mn}_3\text{O}_4$ ; the X-ray diffraction pattern confirmed the formation of this phase. The sample thus obtained at  $400^\circ\text{C}$  shows a change in  $\sigma$  as the temperature is changed. (see cooling and heating cycle in Fig. 1(a)). This behaviour is characteristic of  $\text{Mn}_3\text{O}_4$  and it has tetragonally deformed spinel [16,17].

### 3.1.2. $\text{CdC}_2\text{O}_4 \cdot \text{H}_2\text{O}$

In comparison of thermal analysis (TG and DTA) [7,8] with the conductivity analysis (plot for  $\log \sigma$  against  $T^{-1}$ ) of  $\text{CdC}_2\text{O}_4 \cdot \text{H}_2\text{O}$  in static air atmosphere (Fig. 1(b)) showed the different intermediate phases which occurred during the decomposition. The Region B' and B corresponds to dehydration of  $\text{CdC}_2\text{O}_4 \cdot \text{H}_2\text{O}$  under this atmosphere. The isothermally heated sample under this atmosphere at  $260^\circ\text{C}$ , showed no H–OH band in infrared spectrum and the X-ray diffraction pattern showed broad peaks with a decrease in interplanar spacing. The elemental analysis also agreed well with the anhydrous oxalate ( $\text{CdC}_2\text{O}_4$ ) formation. The value of  $\sigma$  steadily increased from  $352^\circ$  to  $440^\circ\text{C}$  (Region C) and the infrared spectrum of isothermally heated  $\text{CdC}_2\text{O}_4 \cdot \text{H}_2\text{O}$  sample at  $390^\circ\text{C}$  showed a decrease in intensity of coordinated carboxylate bands, in addition bands at  $605\text{ cm}^{-1}$  (m),  $487\text{ cm}^{-1}$  (s) and  $462\text{ cm}^{-1}$  (m) observed for

metal–oxygen stretching frequencies due to presence of CdO [15]. The X-ray diffraction pattern of this isothermally heated sample showed the structure to be polycrystalline in nature, the peaks corresponding to both  $\text{CdC}_2\text{O}_4$  and CdO were observed. The infrared spectrum and X-ray diffraction pattern for the sample decomposed isothermally at  $500^\circ\text{C}$  (Region D) showed mainly CdO. The sample was brown and had an electrical conductivity value of about  $10^{-5}\ \Omega^{-1}\text{ cm}^{-1}$  [18].

It is well known that [6,7] the temperature and the mechanism of the decomposition of oxalate was altered by the surrounding atmosphere. Hence, it is important to compare the data obtained under the atmosphere with the data obtained under different atmospheres.

## 3.2. Dynamic dry nitrogen atmosphere

### 3.2.1. $\text{MnC}_2\text{O}_4 \cdot 2\text{H}_2\text{O}$

Region B in the plot of  $\log \sigma$  against  $T^{-1}$  shown in Fig. 2(a), can be related to dehydration of  $\text{MnC}_2\text{O}_4 \cdot 2\text{H}_2\text{O}$ . Isothermal heating of the parent compound at  $225^\circ\text{C}$  showed its polycrystalline nature as revealed by its X-ray diffraction pattern, and the elemental analysis fitted well to the formula  $\text{MnC}_2\text{O}_4$  [14].

The conductivity plot (Fig. 2(a)) showed a decrease and then steep increase in  $\sigma$  at  $316\text{--}405^\circ\text{C}$  (Region C) and then remained constant above this temperature (Region D). The infrared spectrum and X-ray diffraction pattern of the isothermally heated parent compound in Region C showed that MnO was present together with some  $\text{MnC}_2\text{O}_4$ . Similarly, the infrared spectrum and X-ray diffraction pattern for the sample decomposed isothermally at  $450^\circ\text{C}$  showed mainly MnO; the sample was greyish green. No line which could be assigned to metallic manganese was detected in our work. The sample thus obtained at  $450^\circ\text{C}$  shows a variation in  $\sigma$  with temperature. This behaviour is a characteristic of the non-stoichiometry present in MnO [16,17].

### 3.2.2. $\text{CdC}_2\text{O}_4 \cdot \text{H}_2\text{O}$

Region B' and B in the plot of  $\log \sigma$  against  $T^{-1}$  (Fig. 2(b)), correspond to the dehydration of  $\text{CdC}_2\text{O}_4 \cdot \text{H}_2\text{O}$ . The isothermally heated parent sample at  $240^\circ\text{C}$  under dynamic nitrogen atmosphere was

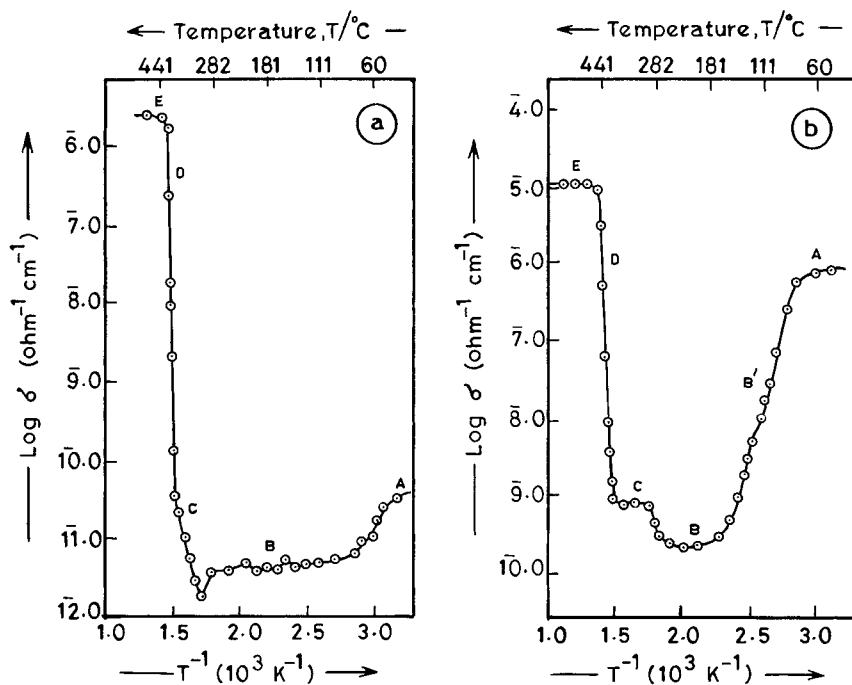


Fig. 2. Plot of  $\log \sigma$  vs.  $T^{-1}$  for (a)  $\text{MnC}_2\text{O}_4 \cdot 2\text{H}_2\text{O}$  and (b)  $\text{CdC}_2\text{O}_4 \cdot \text{H}_2\text{O}$ :  $\odot$ , during decomposition X, cooling cycle.

found to be less crystalline as shown from the X-ray diffraction pattern, while the infrared spectrum showed no H–OH band. The elemental analysis agreed well with the anhydrous compound ( $\text{CdC}_2\text{O}_4$ ).

Further, the conductivity plot showed a steady increase in values of  $\sigma$  in the temperature range 250–380°C (Region C). The infrared spectrum and X-ray diffraction pattern for sample heated isothermally at 360°C showed that CdO was present in this stage together with some  $\text{CdC}_2\text{O}_4$ . A steep increase in  $\sigma$  has been observed in Region D corresponding to CdO formed as the final product. X-ray diffraction analysis has confirmed the formation of this phase.

Although the decomposition behaviour was mostly the same in static air and dynamic dry nitrogen atmospheres some critical differences were observed. These differences could be clarified when the study was carried out under dynamic air atmosphere.

### 3.3. Dynamic air atmosphere

#### 3.3.1. $\text{MnC}_2\text{O}_4 \cdot 2\text{H}_2\text{O}$

The plot of  $\log \sigma$  against  $T^{-1}$  (Fig. 3(a)) showed Region B' and B, indicating dehydration steps.

Further, this plot revealed a definite regions of conductivity corresponding to the various intermediates formed. The isothermal decomposition study under this atmosphere demonstrated that the intermediates were similar to those obtained under the static air atmosphere (see Fig. 1(a)).

#### 3.3.2. $\text{CdC}_2\text{O}_4 \cdot \text{H}_2\text{O}$

Region B in the plot of  $\log \sigma$  against  $T^{-1}$  (Fig. 3(b)) corresponds to the dehydration of  $\text{CdC}_2\text{O}_4 \cdot \text{H}_2\text{O}$ . There was a steady increase in the value of  $\sigma$  between 340° and 410°C (Region C), then there was a steep increase in values of  $\sigma$  in the temperature range 410–510°C (Region D). The infrared and the X-ray diffraction for the sample decomposed isothermally at 380° and 500°C showed CdO along with anhydrous  $\text{CdC}_2\text{O}_4$  and pure CdO, respectively.

The gaseous products obtained by the thermal decomposition of  $\text{MnC}_2\text{O}_4 \cdot 2\text{H}_2\text{O}$  or  $\text{CdC}_2\text{O}_4 \cdot \text{H}_2\text{O}$  under dynamic (pure and dry) nitrogen atmosphere were analysed by qualitative gas detection method. Carbon dioxide was detected by precipitation as calcium carbonate from a solution of calcium hydroxide, while carbon monoxide was detected by reduction of

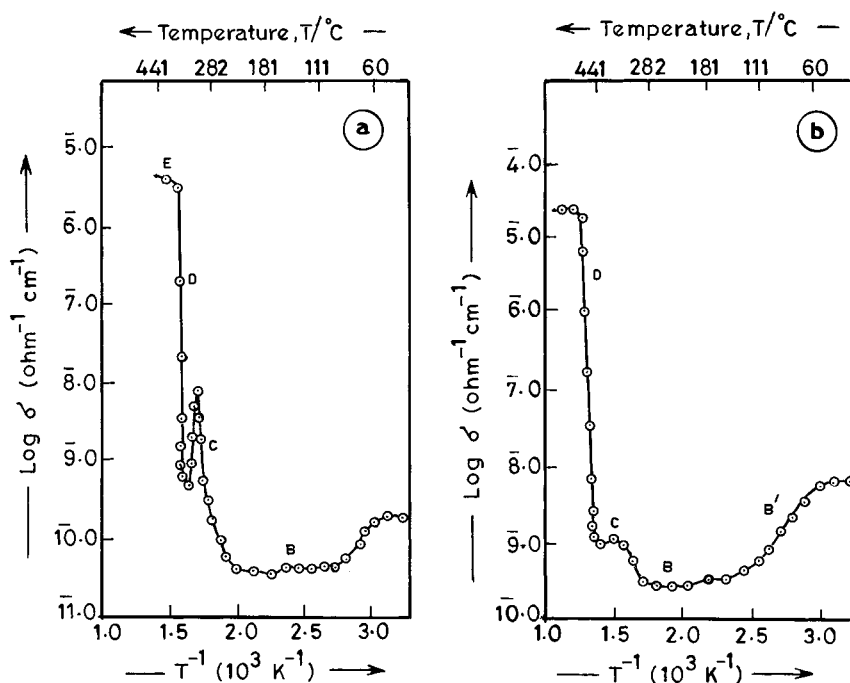
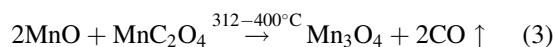
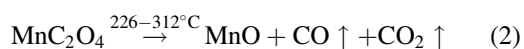


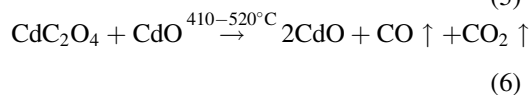
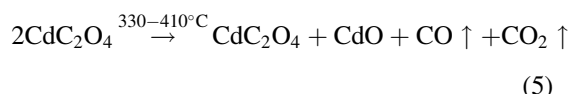
Fig. 3. Plot of  $\log \sigma$  vs.  $T^{-1}$  for (a)  $\text{MnC}_2\text{O}_4 \cdot 2\text{H}_2\text{O}$  and (b)  $\text{CdC}_2\text{O}_4 \cdot \text{H}_2\text{O}$ .

iodine pentoxide into iodine. These gases were also confirmed by gas liquid chromatography (not shown). These chromatograms showed the presence of polar gases (namely  $\text{CO}_2$ ,  $\text{H}_2$  etc. . .). The gases were collected at ca.  $350^\circ\text{C}$ .

The different paths followed by the decomposition of  $\text{MnC}_2\text{O}_4 \cdot 2\text{H}_2\text{O}$  and  $\text{CdC}_2\text{O}_4 \cdot \text{H}_2\text{O}$  in different atmospheres showed complete dehydration, as was seen from conductivity measurements and the infrared spectrum. A transformation of  $\text{MnC}_2\text{O}_4$  to  $\text{MnO}$  was also detected in static and dynamic air atmospheres. A separate phase of  $\text{MnO}$  could not be obtained; this compound always occurred with  $\text{MnC}_2\text{O}_4$ . Thus, the transformation of  $\text{MnO}$  and  $\text{MnC}_2\text{O}_4$  seems to be an equilibrium reaction. This mixture of  $\text{MnO}$  and  $\text{MnC}_2\text{O}_4$  is then transformed to  $\text{Mn}_3\text{O}_4$  which is the final product obtained in static air and dynamic air. These reactions are presented as follows:



The transformation of  $\text{MnC}_2\text{O}_4$  to  $\text{MnO}$  was the final step detected in a dynamic dry nitrogen atmosphere, while  $\text{CdC}_2\text{O}_4$  transformed to  $\text{CdO}$  under static air, dynamic dry nitrogen and dynamic air atmospheres:



#### 4. Conclusions

The present study revealed the following findings on the solid-state dehydration and decomposition of  $\text{MnC}_2\text{O}_4 \cdot 2\text{H}_2\text{O}$  and  $\text{CdC}_2\text{O}_4 \cdot \text{H}_2\text{O}$ .

(a) The oxidative decomposition behaviours of  $\text{MnC}_2\text{O}_4 \cdot 2\text{H}_2\text{O}$  and  $\text{CdC}_2\text{O}_4 \cdot \text{H}_2\text{O}$  were better

understood from the study of the direct current electrical conductivity measurements which showed different regions of conductivity for the intermediates formed.

(b) The final product of decomposition in static air and dynamic air was found to be  $Mn_3O_4$  for  $MnC_2O_4 \cdot 2H_2O$ . However, the final decomposition product in all three atmospheres was found to be CdO for  $CdC_2O_4 \cdot H_2O$ .

## References

- [1] D. Dollimore, J. Dollimore, J. Little, J. Chem. Soc. (1996) 2946.
- [2] M. Brown, D. Dollimore, A.K. Galwey, J. Chem. Soc. Faraday Trans. I 70 (1974) 1316.
- [3] D. Dollimore, J. Therm. Anal. 11 (1977) 185.
- [4] D. Dollimore, Thermochim. Acta 117 (1987) 331.
- [5] X. Ga, D. Dollimore, Thermochim. Acta. 215 (1993) 47.
- [6] E.D. Macklen, J. Inorg. Nucl. Chem. 30 (1968) 2689.
- [7] D. Dollimore, D.L. Griffiths, D. Nicholson, J. Chem. Soc. (1963) 2617.
- [8] C. Duval, Inorganic Thermogravimetric Analysis, Elsevier, Amsterdam, 1953, p. 531.
- [9] D. Dollimore, D. Nicholson, J. Chem. Soc. A (1962) 960.
- [10] R. David, Bull. Soc. Chim. Fr. (1960) 719.
- [11] J.R. Allan, N.D. Baird, A.L. Kassyk, J. Therm. Anal. 16 (1979) 79.
- [12] K.S. Rane, A.K. Nikumbh, A.J. Mukhedkar, J. Mater. Sci. 16 (1981) 2387.
- [13] A.K. Nikumbh, A.E. Athare, V.B. Raut, Thermochim. Acta 186 (1991) 217.
- [14] J. Robin, Bull. Soc. Chim. Fr. (1953) 1078.
- [15] N.T. Mcdevitt, L.B. William, Spectro. Chemica. Acta. 20 (1964) 799.
- [16] D.J. Craik, Magnetic Oxides, vol. 1, Wiley Interscience, New York, 1975, pp. 450, 466.
- [17] K. Fueki, J.B. Wagner, J. Electrochem. Soc. 112 (1965) 970.
- [18] J.C. Bailar, H.J. Emeleus, Sir. R. Nyholm, A.F. Trotman-Dickenson, Comprehensive Inorganic Chemistry, vol. 3, Pergamon Press, 1973, p. 266.